Acute glucose-lowering and insulin-sensitizing action of FGF21 in insulin-resistant mouse models –– association with liver and adipose tissue effects

Jing Xu, Shanaka Stanislaus, Narumol Chinookoswong, Yvonne Y. Lau, Todd Hager, Jennifer Patel, Hongfei Ge, Jen Weiszmann, Shu-Chen Lu, Melissa Graham, Jim Busby, Randy Hecht, Yue-Sheng Li, Yang Li, Richard Lindberg and Murielle M. Véniant

You might find this additional info useful...

This article cites 25 articles, 9 of which can be accessed free at:
http://ajpendo.physiology.org/content/297/5/E1105.full.html#ref-list-1

This article has been cited by 2 other HighWire hosted articles

The lighter side of BDNF
Emily E. Noble, Charles J. Billington, Catherine M. Kotz and ChuanFeng Wang
Am J Physiol Regul Integr Comp Physiol, May , 2011; 300 (5): R1053-R1069.
[Abstract] [Full Text] [PDF]

Thermogenic Activation Induces FGF21 Expression and Release in Brown Adipose Tissue
Elayne Hondares, Roser Iglesias, Albert Giralt, Frank J. Gonzalez, Marta Giralt, Teresa Mampel and Francesc Villarroya
J. Biol. Chem., April 15, 2011; 286 (15): 12983-12990.
[Abstract] [Full Text] [PDF]

Updated information and services including high resolution figures, can be found at:
http://ajpendo.physiology.org/content/297/5/E1105.full.html

Additional material and information about *AJP - Endocrinology and Metabolism* can be found at:
http://www.the-aps.org/publications/ajpendo

This infomation is current as of May 18, 2011.

Acute glucose-lowering and insulin-sensitizing action of FGF21 in insulin-resistant mouse models—association with liver and adipose tissue effects

Jing Xu,[1] Shanaka Stanislaus,[1] Narumol Chinookoswong,[1] Yvonne Y. Lau,[2] Todd Hager,[2] Jennifer Patel,[1] Hongfei Ge,[1,4] Jen Weiszmann,[1,4] Shu-Chen Lu,[1] Melissa Graham,[1] Jim Busby,[1] Randy Hecht,[3] Yue-Sheng Li,[3] Yang Li,[1,4] Richard Lindberg,[1] and Murielle M. Véniant[1]

Departments of [1]Metabolic Disorders, [2]Pharmacokinetics and Drug Metabolism, and [3]Protein Sciences, Amgen Inc., Thousand Oaks; and [4]Amgen Inc., South San Francisco, California

Xu J, Stanislaus S, Chinookoswong N, Lau YY, Hager T, Patel J, Ge H, Weiszmann J, Lu SC, Graham M, Busby J, Hecht R, Li YS, Li Y, Lindberg R, Véniant MM. Acute glucose-lowering and insulin-sensitizing action of FGF21 in insulin-resistant mouse models—association with liver and adipose tissue effects. *Am J Physiol Endocrinol Metab* 297: E1105–E1114, 2009. First published August 25, 2009; doi:10.1152/ajpendo.00348.2009.—Recombinant fibroblast growth factor (FGF)21 has antihyperglycemic, antihyperlipidemic, and antiobesity effects in diabetic rodent and monkey models. Previous studies were confined to measuring steady-state effects of FGF21 following subchronic or chronic administration. The present study focuses on the kinetics of biological actions of FGF21 following a single injection and on the associated physiological and cellular mechanisms underlying FGF21 actions. We show that FGF21 resulted in rapid decline of blood glucose levels and immediate improvement of glucose tolerance and insulin sensitivity in two animal models of insulin resistance (*ob/ob* and DIO mice). In *ob/ob* mice, FGF21 led to a 40–60% decrease in blood glucose, insulin, and amylin levels within 1 h after injection, and the maximal effects were sustained for more than 6 h despite the 1- to 2-h half-life of FGF21. In DIO mice, FGF21 reduced fasting blood glucose and insulin levels and improved glucose tolerance and insulin sensitivity within 3 h of treatment. The acute improvement of glucose metabolism was associated with a 30% reduction of hepatic glucose production and an increase in peripheral glucose turnover. FGF21 appeared to have no direct effect on ex vivo pancreatic islet insulin or glucagon secretion. However, it rapidly induced typical FGF signaling in liver and adipose tissues and in several hepatoma-derived cell lines and differentiated adipocytes. FGF21 was able to inhibit glucose release from H4IIE hepatoma cells and stimulate glucose uptake in 3T3-L1 adipocytes. We conclude that the acute glucose-lowering and insulin-sensitizing effects of FGF21 are potentially associated with its metabolic actions in liver and adipose tissues.

fibroblast growth factor 21; blood glucose; insulin; signal transduction; hepatic glucose production

TYPE 2 DIABETES HAS BECOME an increasing health concern due to its growing incidence worldwide and its serious consequences in morbidity, mortality, and cost to the health care system (24). Recently, fibroblast growth factor 21 (FGF21) has been evaluated as a potential treatment for type 2 diabetes (3, 10).

FGF21 is one of the 22 members of the FGF superfamily (7). Although the majority of the FGF family members are mitogens that stimulate cell proliferation and differentiation, FGF21 lacks mitogenic activity and plays an important role in the regulation of glucose, lipid, and energy homeostasis (2, 5, 11, 21). FGF21 is predominantly expressed in organs related to metabolism, such as liver and pancreas, and is secreted into the bloodstream (5, 16). The expression and circulating levels of FGF21 are subject to nutritional regulation and are elevated during fasting (6). On the basis of in vitro characterizations, FGF21 acts through a signaling receptor complex composed of the coreceptor βklotho and a tyrosine kinase FGF receptor (9, 17, 26). The activity of FGF21 has been shown to stimulate GLUT1 expression and increase GLUT1-mediated glucose uptake in adipocytes (11). FGF21 has also been shown to affect lipolysis in adipose tissues (1, 6), inhibit fatty acid and triglyceride synthesis in liver (25), and preserve β-cell mass and restore β-cell function in the pancreas (22).

Pharmacological studies with recombinant FGF21 have been conducted in a variety of rodent and primate models, including *ob/ob, db/db,* and diet-induced obese (DIO) mice, ZDF rats, and diabetic rhesus monkeys (11, 12, 25). Systemic administration of FGF21 resulted in striking improvement in metabolic parameters, including sustained decreases in circulating glucose and lipid levels and improvement of glucose tolerance and insulin sensitivity (11, 12, 25). Moreover, FGF21 also modulated energy metabolism by increasing energy expenditure and therefore reversed obesity and hepatosteatosis (25). Results from recombinant protein studies were generally in agreement with the phenotypes of FGF21-transgenic mice (11). Mice that overexpressed FGF21 were lean and protected from age-associated or diet-induced obesity and insulin resistance.

Despite well-established metabolic actions of FGF21, previous studies were all confined to measuring the steady-state effects of FGF21 after subchronic or chronic administration of recombinant FGF21 protein or after transgenic overexpression throughout the development. Limited information is available on the kinetics of the biological actions of FGF21. Therefore, the current study investigates the onset, conclusion, and temporal relationships of the biological effects of FGF21 following a single injection. We also examined the physiological and cellular mechanism underlying the observed effects. Two animal models of insulin resistance, (*ob/ob* and DIO mice), were used to determine the metabolic effects of FGF21 after a single injection. In addition, the potential cellular mechanism was also explored ex vivo or in cultured cells.

MATERIALS AND METHODS

Preparation of recombinant human FGF21. Recombinant human FGF21 (amino acids 29–209 without signal peptide) was prepared as

previously described (26). Briefly, recombinant human FGF21 was expressed in *Escherichia coli*. It was then folded in solubilized inclusion bodies and purified by ion exchange and hydrophobic interaction chromatography to obtain >90% purity.

Pharmacokinetics of FGF21 in mice. FGF21 was administered to male C57BL/6 mice as a single intravenous (iv) administration of 0.1, 1, or 10 mg/kg and as a single subcutaneous (sc) or intraperitoneal (ip) administration of 1 mg/kg. Blood samples were obtained at *time 0* (predose), 0.1, 0.25, 0.5, 1, 2, 3, 4, 6, and 12 h after administration from each dose group, with three mice per time point for the determination of serum FGF21 levels. Pharmacokinetic parameters were estimated from serum concentration data via a noncompartmental analysis using WinNonlin Professional software (version 4.1e; Pharsight, Mountain View, CA). The initial concentration at *time 0* after iv administration (C_0) was estimated by back-extrapolation of the first two observed declining concentration values to *time 0*. Maximum concentration after sc or ip administration, C_{max}, and the time maximum concentration occurred (t_{max}) were recorded as observed. Area under the concentration-time curve (AUC) was estimated using the linear/logarithmic trapezoidal method (for the up/down portions of the curve, respectively) up to the last measured concentration that was above the lower detection limit. This area was extrapolated to infinity (AUC_{0-inf}) by the addition of the last measured concentration divided by the apparent terminal disposition rate constant λ_z, as determined by linear regression analysis of the terminal portion of the log serum concentration-time curve. The terminal half-life ($t_{1/2,z}$) was estimated from the terminal rate constant as $\ln(2)/\lambda_z$. Bioavailability (F) after sc or ip administration was calculated as

$$ F(\%) = \frac{AUC_{0-inf,\ SC\ or\ IP}}{AUC_{0-inf,\ IV}} \times \frac{Dose_{IV}}{Dose_{SC\ or\ IP}} \times 100 $$

$AUC_{0-inf,iv}$ value was estimated as $Dose/CL_{av}$, where CL_{av} was the average of the clearance values across animals in iv groups.

FGF21 ELISA assay. The concentrations of immunoreactive FGF21 in serum samples were determined by a sandwich ELISA developed in house. The murine anti-human FGF21 monoclonal antibodies used as capture and detection reagents were also generated internally. The specificity of the antibodies was verified, and the antibodies were shown to react specifically with human FGF21, with no cross-reactivity to murine FGF21. The reactivity of the antibodies to human FGF21 was confirmed by Western blot analysis. The capture antibody was also tested in immunoprecipitation studies and was able to pull down human FGF21 from mouse plasma samples. The linearity of the ELISA assay was determined. Dilutions of an FGF21-spiked sample were recovered within ±10% relative to expected concentration. Linear regression analysis of measured vs. the expected concentration yielded a correlation coefficient of >0.99.

A murine anti-human FGF21 monoclonal antibody was used as the capture antibody bound onto a 96-well plate. Standards and quality controls were prepared for human FGF21 by spiking the test article into 100% C57BL/6 mouse serum. Standards, quality controls, matrix blank, and unknown samples were loaded into the wells after pretreatment in assay buffer. After 2 h incubation followed by washing, a horseradish peroxidase (HRP)-conjugated murine anti-human FGF21 monoclonal antibody prepared in assay buffer was added to the wells as the secondary antibody. After a final wash, a high-sensitivity luminescent peroxidase substrate was added to the wells. In the presence of HRP, a luminescent signal was produced that was proportional to the amount of FGF21 bound by the capture antibody. The intensity of the luminescent signal was measured using a luminometer. The conversion of relative luminescent units to concentration for the unknown samples was achieved through a software-mediated comparison to a standard curve assayed on the same plate. The data underwent regression analysis using the Watson (version 7.0.0.01; Thermo Fisher Scientific) data reduction package.

FGF21 acute metabolic effects in ob/ob mice. All experiments were approved by the Institutional Animal Care and Use Committee of Amgen, Inc. Male *ob/ob* mice were ordered from Jackson Laboratories (cat. no. 000632 B6.V-*Lep*^{ob}/J; Bar Harbor, Maine) at 6 wk of age. Mice were housed five per cage with free access to drinking water and rodent chow. Mice were allowed to acclimate to a 12:12-h light-dark cycle, housing humidity and temperature, and routine restraints and handling for 2 wk before the initiation of the experiment. On the day of the experiment, blood was sampled from the retroorbital sinus of nonanesthetized mice to measure blood glucose as a baseline value (0 h) with a One Touch Glucometer (LifeScan, Milpitas, CA). Mice were then randomized into vehicle or treatment groups to obtain comparable baseline average blood glucose levels. In the first experiment, vehicle, 10 U/kg insulin, or FGF21 dose of 1 or 5 mg/kg was ip injected into *ob/ob* mice. Blood glucose was measured at 1, 3, 6, and 24 h after injection. In a second independent experiment, a broad-range dose-response study for FGF21was conducted. Vehicle or FGF21 dose of 0.01, 0.1, 1, or 3 mg/kg was ip injected into *ob/ob* mice. Blood glucose was measured at 3, 6, 9, and 24 h after injection. In a third experiment, an ip glucose tolerance test (IPGTT) was conducted in *ob/ob* mice. Mice were injected with vehicle or 10 mg/kg FGF21 at 9:00 AM. Food was removed after injection. The IPGTT was initiated 3 h later with a bolus glucose (50% dextrose; Hospira, NDC) injection at a dose of 2 mg/kg. Blood glucose was measured at 0 (before glucose injection), 30, and 90 min after glucose injection.

In a fourth experiment, plasma insulin, glucagon, and amylin were measured at the same time points when blood glucose levels were determined (1, 3, 6, and 24 h) after a single ip injection of vehicle or FGF21 at 1 or 10 mg/kg. For this purpose, ~75 µl of blood was collected from the retroorbital sinus at each indicated time point. Blood glucose was measured with a One Touch Glucometer, and the rest of the blood samples were centrifuged at 6,000 *g* for 10 min to collect plasma. Plasma insulin, glucagon, and amylin were measured using a mouse endocrine multiplex assay (Linco Research, St. Charles, MO).

FGF21 acute metabolic effects in DIO mice. DIO mice were prepared by feeding 4-wk-old male C57BL/6 mice a high-fat diet that contained 60% of energy from fat enriched with saturated fatty acids (D12492; Research Diets, New Brunswick, NJ). After 12 wk of high-fat diet feeding, body weight and blood glucose levels were measured. DIO mice with body weight >40 g and blood glucose level >140 mg/dl were selected and randomized into vehicle or treatment groups to achieve similar baseline average blood glucose levels and body weight between groups.

For the IPGTT experiment, DIO mice were fasted from 9:00 PM to 9:00 AM the next day. Vehicle or 10 mg/kg FGF21 was ip injected at 6:00 AM. Three hours later, an IPGTT was conducted following the same protocol described in the *ob/ob* section.

An independent 2-h hyperinsulinemic-euglycemic clamp study was conducted in DIO mice folowing a 3-h treatment. Briefly, before (4–5 days) a hyperinsulinemic-euglycemic clamp was performed, mice were anesthetized with an ip injection of ketamine (100 mg/kg body wt) and xylazine (10 mg/kg body wt), and an indwelling catheter was inserted into the right jugular vein, after which the mice were allowed to recover. On the day of the clamp experiment, a three-way connector was attached to the jugular vein catheter for iv delivery of glucose or insulin, and blood samples were obtained from the tail vessels. DIO mice were fasted for 12 h (9:00 PM to 9:00 AM) and injected with vehicle or 10 mg/kg FGF21 at 6:00 AM. Three hours after drug administration (9:00 AM), a hyperinsulinemic-euglycemic clamp was initiated with a primed (150 mU/kg body wt) and continuous infusion of human insulin (Humulin; Eli Lilly, Indianapolis, IN) at a rate of 15 pmol·kg^{-1}·min^{-1} to raise plasma insulin within a physiological range. Blood samples (20 µl) were collected at 10- to 20-min intervals for the immediate measurement of plasma glucose concentrations, and 20% glucose was infused at variable rates to maintain glucose at basal

concentrations. Basal and insulin-stimulated whole body glucose turnovers were estimated with a continuous infusion of [3-^{3}H]glucose (PerkinElmer Life and Analytical Sciences, Boston, MA) for 2 h before the clamps (0.05 μCi/min) and throughout the clamps (0.1 μCi/min), respectively. All infusions were performed using microdialysis pumps (CMA Microdialysis, North Chelmsford, MA). To estimate insulin-stimulated glucose uptake in individual tissues, 2-deoxy-D-[1-^{14}C]glucose (2-[^{14}C]DG; PerkinElmer) was administered (10 μCi) 75 min after the start of the clamps. Blood samples were taken before, during, and at the end of clamps for measurement of plasma [^{3}H]glucose, ^{3}H$_2$O and 2-[^{14}C]DG concentrations, and/or insulin concentrations. At the end of the clamp, tissues (gastrocnemius, tibialis anterior, and quadriceps muscles, white and brown adipose tissues, liver, and heart) were taken for biochemical analysis as previously described (13).

Rates of basal hepatic glucose production (HGP) and insulin-stimulated whole body glucose turnover were determined as the ratio of the [^{3}H]glucose infusion rate to the specific activity of plasma glucose at the end of the basal period and during the final 30 min of the clamp, respectively. Insulin-stimulated rates of HGP during the clamp were determined by subtracting the glucose infusion rate from whole body glucose uptake. Whole body glycolysis rates were calculated from the rate of increase in plasma ^{3}H$_2$O concentration, determined by linear regression of the measurements at 80, 90, 100, 110, and 120 min. Whole body glycogen plus lipid synthesis rates were estimated by subtracting the whole body glycolysis rate from whole body glucose turnover rates. Organ-specific glucose uptake rates were calculated from the plasma 2-[^{14}C]DG decay profile and intracellular 2-[^{14}C]deoxyglucose 6-phosphate content.

Mouse islet isolation and hormone secretion studies. Mouse pancreatic islets were isolated by a modification of the collagenase digestion technique described by Lacy and Kostianovsky (15). Briefly, the abdominal cavity was exposed, the common bile duct was cannulated, and the pancreas was filled with 3 ml of cold digestion buffer composed of Hank's balanced salt solution (cat. no. 14065-056; Invitrogen, Carlsbad, CA) supplemented with 25 mM HEPES, 100 μg/ml DNAse I (cat. no. 10 104 159 001; Roche Diagnostics, Mannheim, Germany) and 0.6 mg/ml collagenase, type XI (cat. no. C7657; Sigma-Aldrich, St. Luis, MO). The distended pancreas was excised, moved to a tube containing 5 ml of digestion buffer, and incubated at 37°C for 12 min. The digest was filtered through gauze and washed threetimes in Hanks' balanced salt solution containing 10% fetal bovine serum. Islets were then purified by centrifugation at 1,000 *g* for 30 min at 4°C on a discontinuous gradient prepared from equal volumes of Histopaque 1.119 g/l and 1.077 g/l (cat. no. 1077-1 and 1119-1, Sigma-Aldrich). Purified islets, which were located at the buffer-Histopac 1.077 interface, were collected and washed twice in Hanks' balanced salt solution. The islets were then transferred to RPMI 1640 medium (cat. no. 99-595-CM; Callegro, Manassas, VA) supplemented with 10% fetal bovine serum and 2 mM glutamine and incubated at 37°C for 48 h before secretion studies were performed. For the hormone secretion assay, 10 handpicked, size-matched islets were transferred to 24-well inserts (cat. no. 351184; HTS Multiwell Insert System, Becton-Dickinson, Franklin Lakes, NJ) and incubated for 1 h in oxygenated Krebs-Ringer bicarbonate buffer, pH 7.4, supplemented with 2 mM glutamine, 2 mM arginine, 2 mM alanine, 0.625% human serum albumin, and 1 mM glucose. Islets were then transferred to fresh buffer containing 1 or 10 mM glucose with or without FGF21 (1μg/ml). After a 1-h incubation at 37°C, islets were removed, and the incubation buffer was used to measure insulin and glucagon contents using the Mouse Endocrine Lincoplex kit (cat. no. MENDO-75K; Millipore, St. Charles, MO).

Cell cultures and adipocyte differentiation. The rat hepatoma cell lines FAO and H4IIE, the human hepatoma line HepG2, and 3T3-L1 fibroblasts were obtained from the American Type Culture Collection (Rockville, MD). The FAO cells were maintained in Coon's modified Ham's F12 medium supplemented with 10% FBS and 2 mM L-

glutamine, and the other cells were maintained in DMEM with the same supplements. 3T3-L1 fibroblasts were induced to differentiation by adding 250 nM dexamethasone (Sigma D4902), 500 mM isobutylmethylxanthine (Sigma I7018), and 1 mg/ml insulin (Sigma I9278) into basic culture medium for 2 days. The cells were then cultured in DMEM with 10% FBS, 1% Pen-Strep, and 1 mg/ml insulin for 2 days and in basic culture medium for an additional 3 days thereafter. Human subcutaneous preadipocytes and postdifferentiated adipocytes were purchased from Zen-Bio (Research Triangle Park, NC) and were maintained in Zen-Bio preadipocyte (cat. no. PM-1) and adipocyte medium (DM-2-500), respectively.

FGF21 signaling, western blot analysis, and ELISA-MSD assay. Cells cultured on multiwell plates were serum starved and treated with recombinant FGF21 at indicated concentrations for 10–15 min. In a study conducted in HepG2 and FAO cells, heparin (cat. no. H3393, Sigma) at 1 μg/ml concentration was added to test whether heparin could potentiate FGF21 signaling. The cells were then harvested and snap-frozen in liquid nitrogen. Male C57BL6 mice were ip injected with vehicle, 50 U/kg insulin, or 10 mg/kg FGF21. Fifteen minutes after injection, liver, epididymal white adipose tissue, heart, and gastrocnemius skeletal muscle were collected and snap-frozen in liquid nitrogen. Whole cell or tissue lysates were prepared in lysis buffer (30 mM Tris·HCl pH 7.4, 150 mM NaCl, 0.5 mM EDTA, 10% glycerol, 1% NP-40, 0.5 mM PMSF, 1 mM NaVO$_3$, 40 mM NaF). The lysates containing 25 μg of protein were subjected to Western blot analysis and ELISA-MSD assays respectively.

The following antibodies were used in Western blot analysis: anti-βklotho antibody (cat. no. AF2619, A&D System, Minneapolis, MN), anti-phospho-FRS-2 (FGF receptor substrate 2; Tyr^{196}) antibody (cat. no. 3864, Cell Signaling, Denver, MA); anti-phospho-ERK1/2 (Thr^{202}/Tyr^{204}) antibody (cat. no. 9101, Cell Signaling), and anti-total ERK1/2 antibody (cat. no. 9102, Cell Signaling). The ELISA-MSD assays were independently used to measure total and phosphorylated ERK1/2 (Thr^{202}/Tyr^{204}) (cat. no. K11107D-2; Meso Scale Discovery, Gaithersburg, MD) and total and phosphorylated Akt (Ser^{473}) (cat. no. K11100D-2; Meso Scale Discovery, Gaithersburg, MD) in tissue lysates following the assay kit's protocol. The signal was detected using SECTOR imager 6000 (Meso-Scale Discovery). Data were expressed as the percentage of phosphorylated ERK1/2 or Akt in relative to total ERK1/2 or Akt (p-ERK/total ERK) × 100 or (p-Akt/total Akt) × 100.

Glucose production assay in H4IIE cells. Subconfluent H4IIE cells were plated at 100,000 cells/well in 96-well tissue culture plates in 100 μl of growth medium (DMEM with 10% FBS) and left to attach for ~3 h. The growth medium was removed, and the cells were washed in 100 μl of phosphate-buffered saline. Excess phosphate-buffered saline was removed, 100 μl of glucose production medium (glucose- and serum-free DMEM containing 20 mM sodium lactate and 2 mM sodium pyruvate) was added, and cells were left overnight at 37°C in 5% CO$_2$. The following day, the medium was replaced with 90 μl of fresh glucose production medium. Dilutions of compounds and insulin were performed in glucose production medium, and a 10-μl volume was added to the cells. The treated cells were left overnight, and the following day the medium was recovered and either it was frozen or glucose production was measured immediately using the Amplex Red glucose assay kit (A22189, Invitrogen) according to the manufacturer's instructions.

Glucose uptake assay in differentiated 3T3-L1 adipocytes. Seven days after differentiation, 3T3-L1 adipocytes were washed once with DMEM containing 1% FBS and 1% Pen-Strep. FGF21 and FGF23 were added to the adipocytes at the indicated concentrations in DMEM with 1% FBS and 1% Pen-Strep, and the adipocytes were incubated for 72 h at 37°C. The cells were then washed once with glucose-free DMEM (Invitrogen 11966–025) containing 0.1% fatty-acid free BSA (Sigma A9205) and FGF21 and FGF23 were added to the cells at the indicated concentrations in the same medium. After 2.5 h of incubation, insulin was added at the indicated concentrations

to wells containing glucose-free DMEM and 0.1% fatty acid-free BSA, and the cells were incubated for an additional 30 min. The cells were then washed twice with Krebs-Ringer phosphate buffer (KRP) composed of 118 mM NaCl, 4.8 mM KCl, 1.3 mM $CaCl_2$, 1.2 mM KH_2PO_4, 1.2 mM $MgSO_4$ and 15 mM HEPES (pH 7.4), with 0.1% fatty acid-free BSA added. Cells were treated with FGF21, FGF23, or insulin at the indicated concentrations in KRP containing 0.1% fatty acid-free BSA. 2-[1-^{3}H]DG (Sigma 322091) was added to the cells at a concentration of 0.2 μCi/well, and they were incubated for 1 h at 37°C. Cytochalasin B (50 μM; Sigma C6762) was added to the cells to terminate the reaction and 2-DG uptake was measured on a Wallac MicroBeta. Nonspecific 2-DG uptake was measured in the presence of 50 μM cytochalasin B and subtracted from each sample to obtain specific uptake.

Statistical analysis. Data are presented as means ± SE. Statistical comparison of the means among the groups was made using one-way ANOVA. Differences between the means of individual groups were analyzed by the post hoc Fisher's test using Statview software (SAS Institute, Cary, NC).

RESULTS

Pharmacokinetics of FGF21 in mice. The pharmacokinetics of FGF21 was characterized in male C57BL/6 mice (Fig. 1). Over a single iv dose range of 0.1, 1, and 10 mg/kg, the pharmacokinetics of FGF21 appeared to be linear, with exposure (C_0 and AUC_{0-inf}) increasing approximately dose proportionally (Fig. 1 and Table 1). The terminal half-life ranged from 1.45 to 1.94 h following iv administration. C_{max} was achieved at 0.1 and 2 h following ip and sc administration, respectively. The bioavailability of FGF21 after a single ip or sc dose of 1 mg/kg was estimated to be 47.8 and 51.1%, respectively. Similar pharmacokinetics of FGF21 was observed in *ob/ob* mice (unpublished observation). The predicted binding affinity of FGF21 to one of its receptors, βklotho, and the in vitro potency of FGF21 in a βklotho-recombinant cell line were reported previously (26).

FGF21 acutely reduced blood glucose levels and improved glucose tolerance in ob/ob mice. The acute glucose-lowering effect of FGF21 was tested in *ob/ob* mice. Insulin, a potent hypoglycemic agent, was included in the same study as a positive control. Vehicle, 10 U/kg insulin, or FGF21 (1 or 5

Table 1. *Mean pharmacokinetic parameters of FGF21 following iv, sc, or ip administration of FGF21 to C57BL/6 mice*

Pharmacokinetic Parameters	0.1 mg/kg iv	1 mg/kg iv	10 mg/kg iv	1 mg/kg sc	1 mg/kg ip
t_{max}, h	NA	NA	NA	2.0	0.1
C_0 or C_{max}, nM	237	1,890	17,200	73.0	77.0
AUC_{0-inf}, nM·h	31.8	443	4,400	187	200
$t_{1/2,z}$, h	1.94	1.50	1.45	1.06	1.30
F,%	NA	NA	NA	47.8	51.1

All data presented are means of 3 mice per group. FGF, fibroblast growth factor; NA: not applicable; C_0, extrapolated serum concentration at *time 0;* C_{max}, maximum serum concentration after sc or ip administration; AUC_{0-inf}, area under the concentration-time curve from zero to infinity; $t_{1/2,z}$, half-life associated with the terminal phase; F (%), bioavailability, relative to mean AUC_{0-inf} of iv dose group

mg/kg) was injected into 8-wk-old *ob/ob* mice. Blood glucose was measured before treatment injection and at various time points following the injection. As expected, insulin reduced blood glucose levels by 50% from baseline at 1 h after injection, and the glucose levels returned to baseline 3 h after injection (Fig. 2A). Interestingly, FGF21 also led to a rapid and sustained decrease in blood glucose levels in *ob/ob* mice. The maximum glucose reduction of 40% from baseline was reached within 1 h after FGF21 injection (Fig. 2A) and was sustained for at least 6 h. The blood glucose levels returned to baseline within 6–24 h (Fig. 2A). The 1 mg/kg dose of FGF21 was a plateau dose, as no further glucose lowering was observed when the FGF21 dose was increased from 1 to 5 mg/kg (Fig. 2A).

A broader dose-response study of FGF21 was subsequently conducted to identify the minimum effective dose. FGF21 was found to be effective in causing a 20–30% glucose drop from baseline at a dose as low as 0.01 mg/kg (Fig. 2B). A dose of 0.1 mg/kg FGF21 led to a maximum glucose reduction of ~60% from baseline in this experiment (Fig. 2B). When the doses were ≥0.1 mg/kg, the glucose-lowering effect of FGF21 was maintained for up to 6 h, then waned between 6 and 9 h, and was finally undetectable at 24 h following injection (Fig. 2, A and B).

An IPGTT was conducted in *ob/ob* mice to test whether FGF21 could acutely improve the tolerance to a glucose challenge. Vehicle or 10 mg/kg FGF21 was injected into 8-wk-old *ob/ob* mice. Food was then removed. Three hours later (*time 0* of the IPGTT), blood glucose levels were statistically significantly lower in FGF21-treated mice (126 ± 10 mg/dl vs. 166 ± 11 mg/dl in FGF21- vs. vehicle-treated mice, respectively, $P < 0.01$; Fig. 2C). There was no statistically significant difference in body weight between vehicle and FGF21 treatment groups (data not shown). A bolus glucose solution was injected at *time 0*. The glucose AUC (data not shown) were statistically significantly reduced in FGF21-treated mice compared with vehicle-treated mice (Fig. 2C).

FGF21 acutely reduced plasma insulin and amylin levels in ob/ob mice. To investigate whether the acute blood glucose-lowering effect of FGF21 was mediated through changes in glucoregulatory hormone levels, we conducted a similar time course study to measure plasma insulin, glucagon, and amylin levels at the same time points for which blood glucose levels were determined (0, 1, 3, 6, and 24 h). For this purpose, a
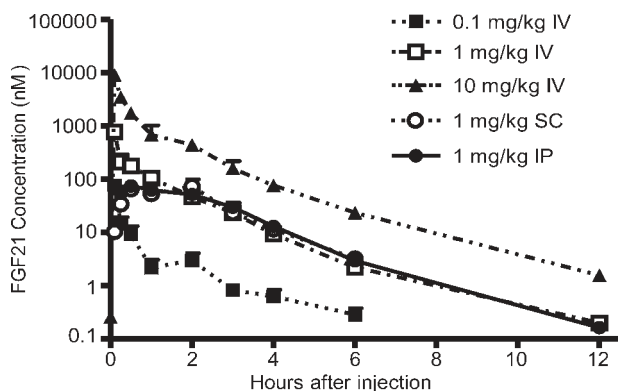

Fig. 1. Serum concentration of fibroblast growth factor 21 (FGF21) over a course of 24 h in C57BL6 male mice. FGF21 was administered to male C57BL/6 mice as a single iv administration of 0.1 (■), 1 (□), and 10 mg/kg (▲) and as a single sc (○) or ip (●) administration of 1 mg/kg. Blood samples were obtained at *time 0* (predose), 0.1, 0.25, 0.5, 1, 2, 3, 4, 6, and 12 h after administration to determine serum FGF21. Data represent means ± SE of 3 animals per time point per group.
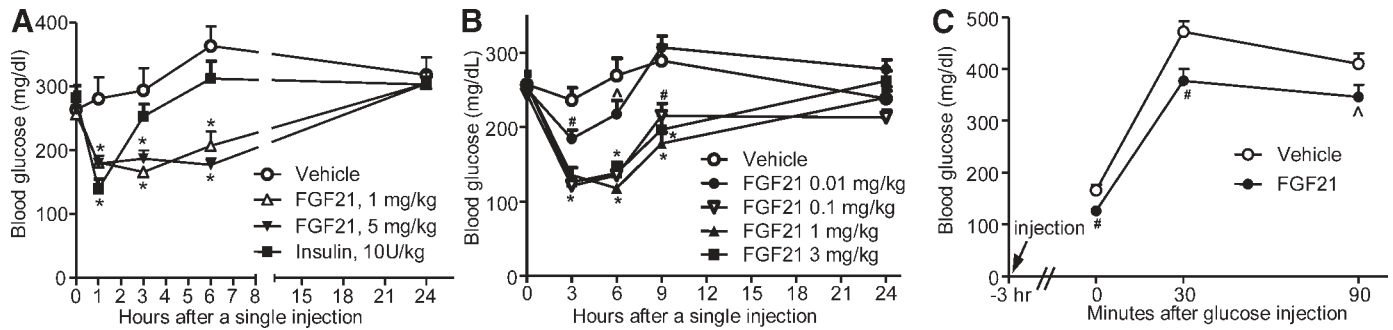
Fig. 2. FGF21 rapidly reduced blood glucose levels and improved glucose tolerance in *ob/ob* mice. *A*: time course of FGF21 and insulin on blood glucose lowering over a 24-h period following a single injection in *ob/ob* mice. ○, vehicle; △, 1 mg/kg FGF21; ▼, 5 mg/kg FGF21; ■, 10 U/kg insulin. *B*: dose-response of FGF21 on blood glucose lowering over a 24-h period following a single injection in *ob/ob* mice. ○, vehicle; ●, 0.01 mg/kg FGF21; ▽, 0.1 mg/kg FGF21; ▲, 1 mg/kg FGF21; ■, 3 mg/kg FGF21. *C*: ip glucose tolerance test (IPGTT) in o*b/ob* mice. Mice were ip injected with vehicle or 10 mg/kg FGF21, food was then removed, and IPGTT was initiated 3 h after injection. Data represent means ± SE; n = 8–10 animals/group. *$P < 0.001$, #$P < 0.01$, ^$P < 0.05$ vs. vehicle-treated mice.

relatively large volume (~75 µl) of blood was serially collected from each mouse from the retroorbital sinus at each indicated time point. Similarly to what is shown in Fig. 2, FGF21 at 1 and 10 mg/kg resulted in a rapid and sustained reduction of blood glucose levels in *ob/ob* mice (data not shown). Interestingly, FGF21 also resulted in a rapid and sustained reduction of plasma insulin and amylin levels, and the temporal change of plasma insulin and amylin levels not only mirrored each other but also paralleled that of blood glucose levels (Fig. 3, *A* and *B*). The maximum reduction of insulin and amylin levels from baseline was 40–50%, which was also observed at 1 h following injection and sustained for

more than 6 h at the 10 mg/kg dose of FGF21. Plasma glucagon levels were not significantly affected by FGF21 treatment (Fig. 3*C*). At 1 h after injection, plasma insulin and amylin levels in vehicle-treated mice also significantly declined from baseline, and the treatment difference in insulin levels at 1 h did not reach statistical significance (Fig. 3, *A* and *B*). The decrease in plasma insulin and amylin levels at 1 h in vehicle-treated mice may be explained by a stress response induced from frequent animal handling at baseline when animals were injected and blood was collected. Therefore, the current blood sampling technique may not have been ideal. More sophisticated techniques that allow frequent blood sam-
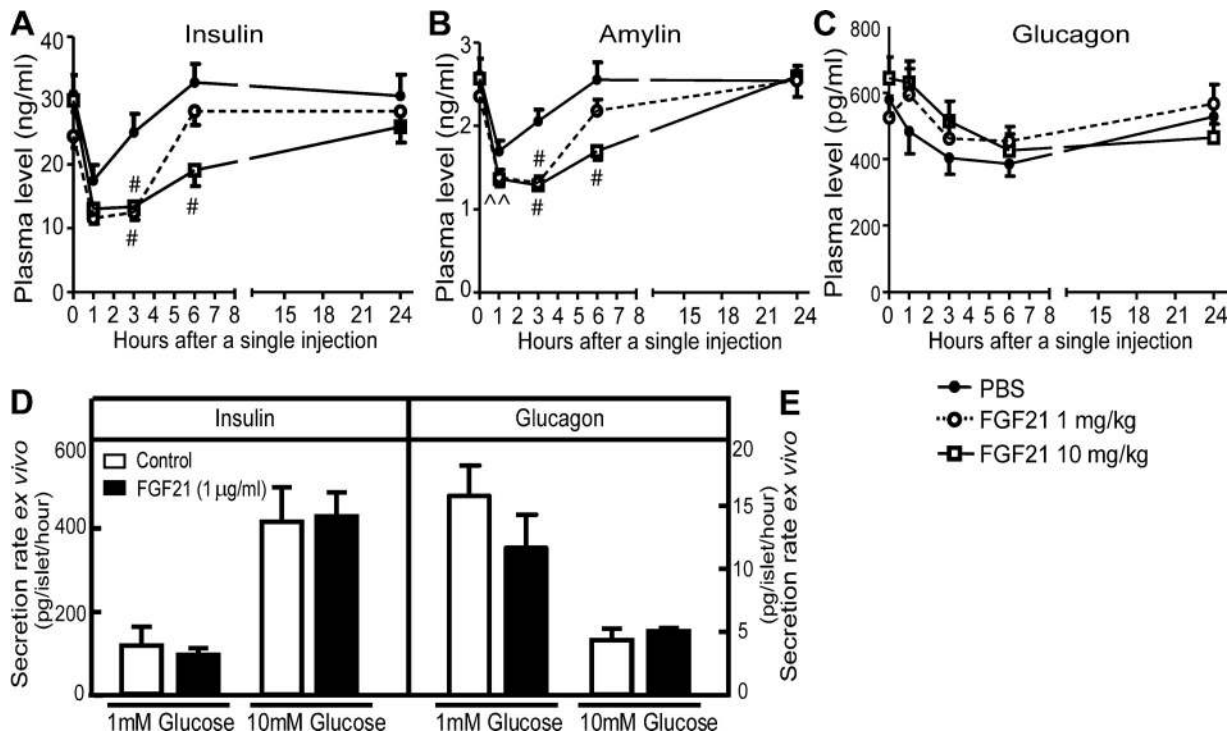

Fig. 3. Effects of FGF21 on plasma hormone levels and islet hormone secretion. *A–C*: following a single injection, FGF21 rapidly reduced plasma insulin (*A*) and amylin levels (*B*) without affecting plasma glucagon levels (*C*) in *ob/ob* mice. Vehicle, ●; 1 mg/kg FGF21, ○; 10 mg/kg FGF21, □. Data represent means ± SE; n = 10–12 animals/group. #$P < 0.01$, ^$P < 0.05$ vs. vehicle-treated mice. *D* and *E*: insulin (*D*) and glucagon secretion (*E*) in cultured mouse pancreatic islets. Mouse pancreatic islets were isolated and incubated in 1 or 10 mM glucose in the presence or absence of FGF21 (1 µg/ml). Culture medium was collected after 1-h incubation to determine insulin and glucagon levels. Data are means ± SE of 4 replicates expressed as pg hormone content·islet^{-1}·h^{-1}.

pling will be necessary to monitor hormonal changes in the future.

To investigate whether FGF21 has a direct role on pancreatic islet insulin and glucagon secretion, isolated mouse islets were treated with FGF21 at low and high concentrations of glucose. As expected, 10 mM glucose stimulated insulin secretion (Fig. 3*D*) and suppressed glucagon secretion (Fig. 3*E*) in cultured islets. The addition of 1 μg/ml FGF21 had no effect on insulin or glucagon secretion in either high- or low-glucose conditions (Fig. 3, *D* and *E*).

FGF21 acutely improved glucose tolerance and insulin sensitivity in DIO mice. We next investigated whether FGF21 could acutely reduce blood glucose and improve glucose metabolism in polygenic obese DIO mice. Similarly to what was observed in *ob/ob* mice, fasting blood glucose levels were statistically significantly reduced after 3 h of treatment with FGF21 in DIO mice (*time 0* of GTT: 148 ± 4 vs. 115 ± 7 mg/dl in vehicle- vs. FGF21-treated mice, respectively, $P <$ 0.01; Fig. 4*A*). In these same mice, glucose tolerance was also significantly improved. Plasma glucose levels were statistically significantly lower at 30 min ($P < 0.05$), 90 min ($P < 0.01$), and 160 min ($P < 0.01$) after a bolus glucose injection in FGF21-treated mice compared with vehicle-treated mice (Fig. 4*A*).

Insulin sensitivity was assessed by performing a hyperinsulinemic-euglycemic clamp study in DIO mice following an FGF21 acute (3-h) treatment. The basal and clamp glucose and insulin levels are shown in Table 2. As was observed with *ob/ob* mice, DIO mice treated with FGF21 for 3 h showed a statistically significant reduction in basal insulin levels (301 ±

Table 2. *Metabolic parameters during basal (12-h fast) and hyperinsulinemic-euglycemic clamp periods in DIO mice receiving a single injection of vehicle or FGF21 3 h prior to the clamp*

			Basal		Clamp	
	n	Body weight, g	Glucose, mg/dl	Insulin, pM	Glucose, mg/dl	Insulin, pM
Vehicle	9	44.7±0.8	227±9	301±33	132±12	376±21
FGF21 (10 mg/kg)	10	45.9±0.8	204±11	116±16*	115±6	347±33

All data represent means ± SE. *$P < 0.001$ vs. vehicle-treated mice.

33 vs. 116 ± 16 pM in vehicle- vs. FGF21-treated mice, respectively, $P < 0.001$; Table 2). A slight reduction in basal fasting blood glucose levels was also observed (227 ± 8.7 vs. 204 ± 11 mg/dl in vehicle- vs. FGF21-treated mice, respectively, $P = 0.115$; Table 2). However, the difference did not reach statistical significance, possibly due to the restraining and handling procedure before the initiation of the insulin clamp. With the insulin infusion, plasma glucose levels were clamped at similar physiological concentrations between vehicle- and FGF21-treated groups (Table 2; 132 ± 12 mg/dl vs 115 ± 6 mg/dl in vehicle- vs FGF21-treated mice, respectively). The glucose infusion rate required to maintain euglycemia was approximately sixfold higher in FGF21-treated mice than in vehicle-treated mice (Fig. 4*B*). The basal hepatic glucose production was not altered by acute FGF21 treatment (Fig. 4*C*). The clamp hepatic glucose production rate was reduced by 32% in FGF21-treated mice, although this change did not

Fig. 4. FGF21 acutely improved glucose tolerance and insulin sensitivity in DIO mice. *A*: IPGTT in 12-h-fasted DIO mice treated with vehicle (○) or 10 mg/kg FGF21 (●) 3 h prior to IPGTT. *B–G*: hyperinsulinemic-euglycemic clamp study in DIO mice treated with vehicle (open bar) or 10 mg/kg FGF21 (filled bar) 3 h prior to initiation of the clamp. *B*: steady-state glucose infusion rate was obtained from averaged rates of 90–120 min of hyperinsulinemic-euglycemic clamps; *C*: basal rates of hepatic glucose production (HGP); *D*: insulin-stimulated rates of HGP during clamps; *E*: insulin-stimulated whole body glucose turnover; *F*: whole body glycolysis; *G*: whole body glycogen plus lipid synthesis. All data represent means ± SE; *n* = 9–10/group. #$P < 0.01$ vs. vehicle-treated mice.
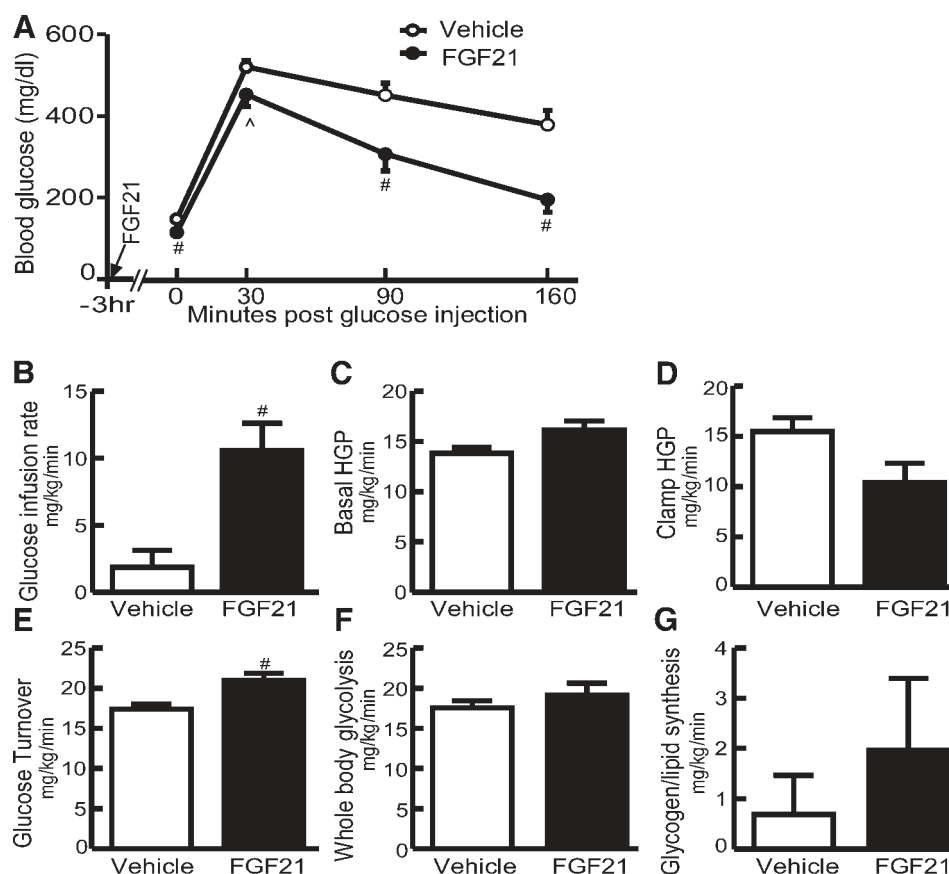
reach statistical significance (Fig. 4*D*). Whole body glucose turnover was statistically significantly elevated in mice treated with FGF21 compared with vehicle-treated mice ($P < 0.01$; Fig. 4*E*). There was no significant treatment-related change in the rate of whole body glycolysis (Fig. 4*F*) or glycogen/lipid synthesis (Fig. 4*G*). The [^{14}C]2-DG uptake was measured in insulin-responsive tissues, including white and brown adipose tissues, heart, and skeletal muscle. None of the tissues examined showed statistically significant increases in glucose uptake [Supplemental Fig. 1 (supplemental material is found in the online version at the Journal website)].

FGF21 stimulated typical FGF signaling in liver and white adipose tissues and in several hepatoma-derived cell lines and differentiated adipocytes. FGF21 has been shown to activate signaling cascades downstream of FGF receptors in a βklotho-dependent manner in vitro. The FGF21-induced signaling events, such as phosphorylation of ERK1/2, could be observed within 2–3 min of treatment and peaked at 10 min when tested in multiple cell types, such as INS-1E β-cell line (22) and 3T3-L1 adipocytes (11). To determine which tissues potentially respond to FGF21 stimulation, we examined the tissue expression pattern of βklotho and the phosphorylation of signaling molecules downstream of FGF receptors following an acute FGF21 injection in vivo. βklotho protein was found to be expressed in liver and adipose tissues and was not detectable in heart and skeletal muscle (Fig. 5*A*). Consistent with the βklotho tissue expression pattern, the typical FGF signaling indicated by the phosphorylation of ERK1/2 was specifically enhanced in liver and adipose tissues 15 min following FGF21

treatment, as shown by Western blot analysis (Fig. 5*B*). In contrast, the phosphorylation of ERK1/2 was not significantly altered in heart and skeletal muscle (Fig. 5*B*). An ELISA-MSD assay was independently conducted to quantify phosphorylated and total ERK1/2 in the tissue lysates. FGF21 increased the percentage of phosphorylated ERK1/2 over total ERK1/2 two- to threefold in liver and adipose tissues (Fig. 5*C*). An ELISA-MSD assay was also conducted to measure phosphorylated and total Akt in response to FGF21 stimulation. FGF21 had minimal effects on Akt phosphorylation in any of the tissues examined (Fig. 5*D*). Insulin was included in the same experiment to compare its signal transduction profile with that of FGF21. As expected, insulin was a weak activator of ERK1/2 but a strong activator of Akt (Fig. 5, *B–D*). Insulin had minimal effects on ERK1/2 phosphorylation in liver and heart (Fig. 5, *B* and *C*). It primarily stimulated phosphorylation of ERK1/2 in muscle (Fig. 5, *B* and *C*), with an intermediate effect in white adipose tissue (Fig. 5*B*). Insulin strongly induced Akt phosphorylation in all the tissues examined (Fig. 5*D*). Therefore, FGF21 and insulin induced different intracellular signaling responses in different tissues, suggesting that the two pathways are distinct from each other, at least upstream of the Akt and ERK1/2 targets.

We next examined whether FGF21 could also induce signaling events in adipocytes and liver-derived cell lines. As previously seen in published results regarding 3T3-L1 adipocytes (11, 17), FGF21 stimulated phosphorylation of FRS-2 and ERK1/2 in human differentiated adipocytes (Fig. 6*A*). The signaling activity was not detectable in undifferentiated human
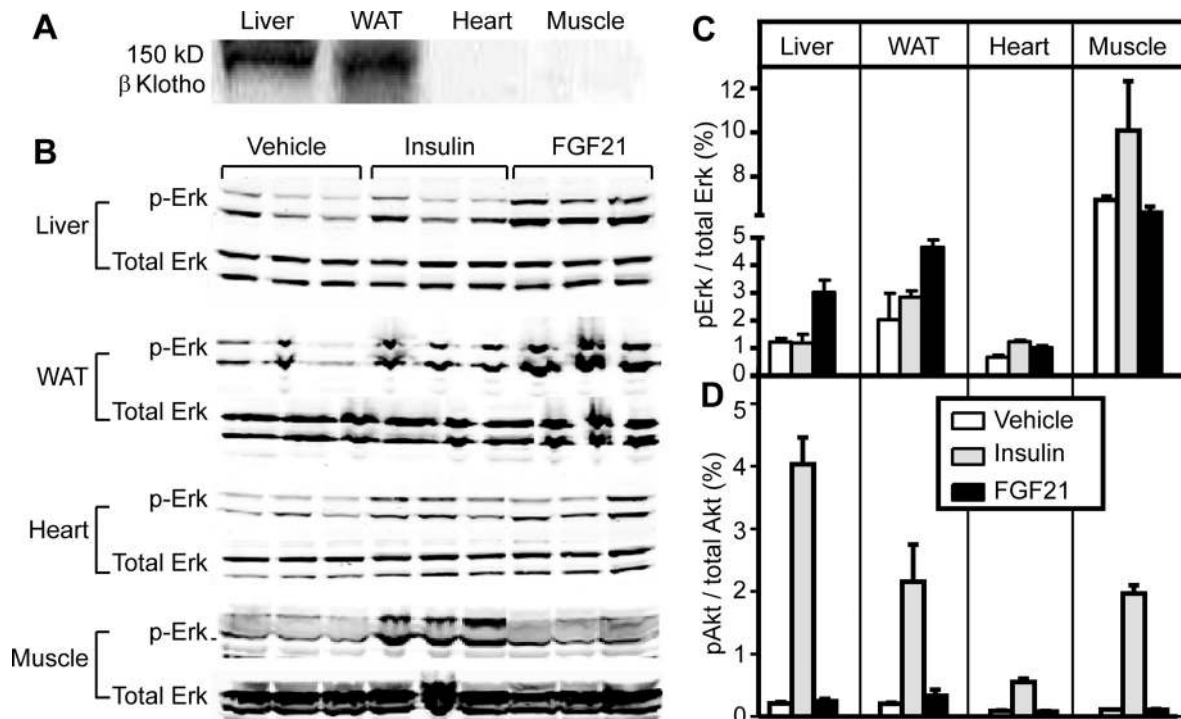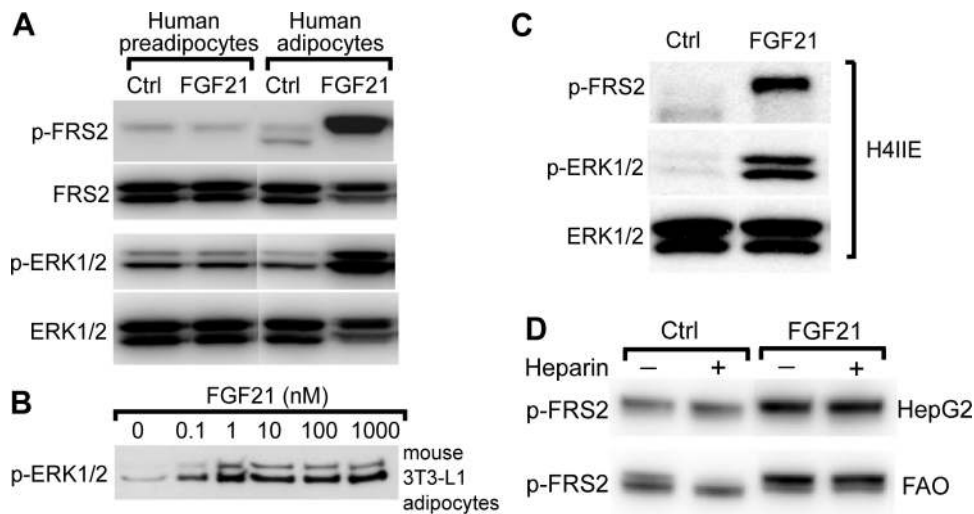
Fig. 5. FGF21 stimulated phosphorylation of ERK1/2 specifically in liver and adipose tissues in C57BL6 mice. *A*: Western blot analysis of βklotho tissue expression in C57B6 mice. Total tissue lysates were prepared and pooled from 4 mice and subjected to Western blot analysis. *B*: C57B6 mice were injected ip with vehicle, 50 U/kg insulin, or 10 mg/kg FGF21. Liver, white adipose tissue (WAT), heart, and skeletal muscle tissues were collected 15 min following injection. Total tissue lysates were prepared and pooled from 3 mice for Western blot analysis. p-Erk, phosphorylated ERK. *C* and *D*: ELISA-MSD assay for p-ERK1/2 and total ERK1/2 (*C*) and p-Akt and total Akt (*D*). Tissue lysates were subjected to ELISA-MSD assays. Data are expressed as percentage of p-ERK1/2 or p-Akt relative to total ERK1/2 or Akt. Open bar:, vehicle; gray bar, 50 U/kg insulin; filled bar, 10 mg/kg FGF21. Data are means ± SE; $n = 3$ per group.

Fig. 6. FGF21 stimulated typical FGF signaling in differentiated adipocytes and hepatoma-derived cell lines. *A*: FGF21 increased phosphorylation of FGF receptor substrate 2 (FRS2) and ERK1/2 in differentiated human sc adipocytes but not in human predifferentiated adipocytes. Cells were starved overnight and then treated with or without 250 nM FGF21 for 10 min. Total cell lysates were prepared and subjected to Western blot analysis. *B*: dose-response of FGF21 on ERK1/2 phosphorylation in differentiated 3T3-L1 adipocytes. *C*: FGF21 (20 nM) stimulated phosphorylation of FRS2 and ERK1/2 in H4IIE rat hepatoma-derived cells. *D*: FGF21 stimulated phosphorylation of FRS2 in HepG2 and FAO hepatoma-derived cell lines. Cells were treated with or without 30 nM FGF21 in the presence or absence of 1 µg/ml heparin for 10 min.

preadipocytes (Fig. 6*A*), possibly due to the lack of βklotho expression in preadipocytes. We also confirmed the previous finding that FGF21 dose-dependently stimulated phosphorlation of ERK1/2 in 3T3-L1 adipocytes (Fig. 6*B*). In addition, FGF21 induced phosphorylation of FRS-2 or ERK1/2 in several human and rat hepatoma-derived cell lines, such as H4IIE (Fig. 6*C*), HepG2 (Fig. 6*D*), and FAO (Fig. 6*D*) cells. Furthermore, the signaling activity of FGF21 appeared not to be potentiated by the addition of heparin (Fig. 6*D*).

FGF21 dose-dependently reduced glucose production in H4IIE cells and stimulated glucose uptake in 3T3-L1 adipocytes. H4IIE hepatoma-derived cells have many properties similar to those of hepatocytes and have been broadly used as

a cellular system to study glucose metabolism and insulin signaling. We tested whether FGF21 could affect glucose production in H4IIE cells. Insulin was used as a positive control. As expected, insulin showed strong inhibition of glucose production with an IC_{50} value of ~60 pM (Fig. 7*A*). Treatment with FGF21 also resulted in a dose-dependent reduction of endogenous glucose production in H4IIE cells, with an IC_{50} value of ~0.8 nM (Fig. 7*B*). We also conducted a dose-response study to evaluate the potency of FGF21 in stimulation of glucose uptake in differentiated 3T3-L1 adipocytes. As expected, insulin used as a positive control showed stimulation of glucose uptake in adipocytes, with an EC_{50} value of ~1.0 nM (Fig. 7*C*). FGF23, a close family member of
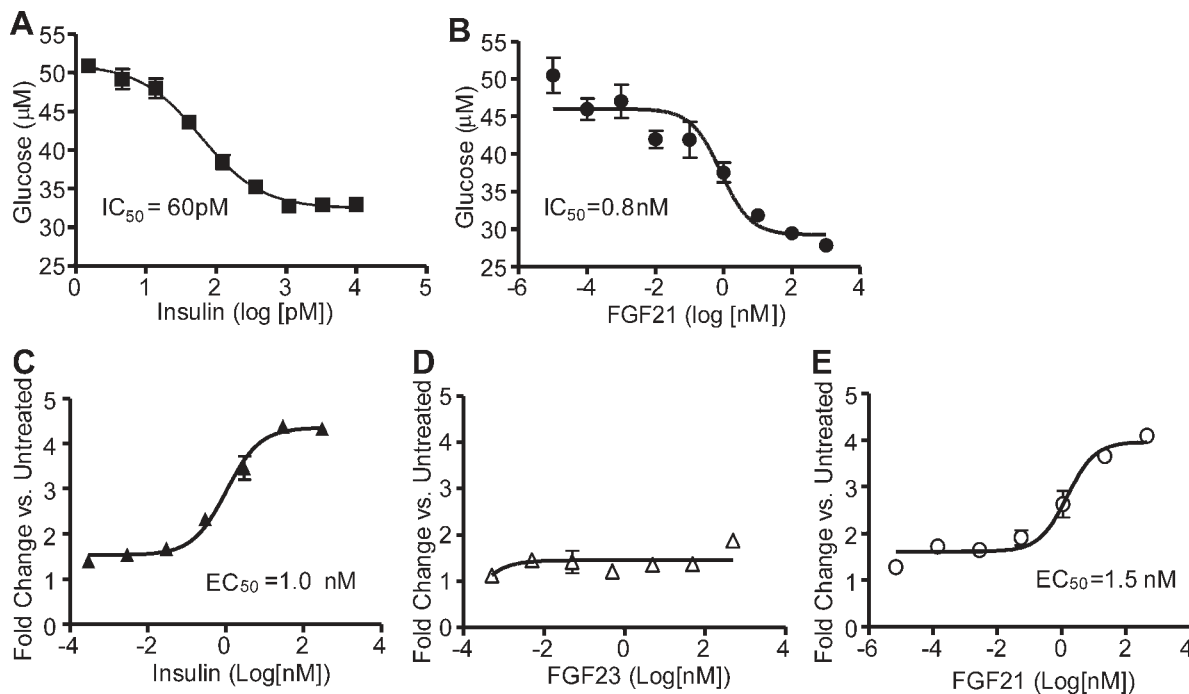

Fig. 7. FGF21 dose-dependently decreased glucose production in H4IIE cells and stimulated glucose uptake in 3T3-L1 adipocytes. *A* and *B*: dose-response curves of insulin (*A*) and FGF21 (*B*) on glucose production in H4IIE cells. *C–E*: dose-response curves of insulin (*C*), FGF23 (*D*), and FGF21 (*E*) on glucose uptake in 3T3L1 adipocytes. Results are expressed as fold change over cells treated with vehicle (10 mM potassium phosphate, 14.0 mM sodium chloride, pH 8.0). All data presented are means of triplicate measurements ± SE; *n* = 3.

FGF21, did not show the ability to stimulate glucose uptake in adipocytes (Fig. 7D), whereas FGF21 increased adipocyte glucose uptake, with an EC_{50} value of ~1.5 nM (Fig. 7E).

DISCUSSION

Despite abundant information relating to the steady-state metabolic effects of FGF21 following subchronic or chronic administration of FGF21 in animal models, limited knowledge is available on the kinetics of the biological action of FGF21 and the associated physiological and cellular mechanisms. Here, we show that FGF21 rapidly reduced blood glucose and insulin levels and improved glucose tolerance and insulin sensitivity in two separate insulin-resistant animal models (*ob/ob* and DIO mice). FGF21 appeared to have no direct effect on pancreatic islet insulin or glucagon secretion. The rapid onset of glucose-lowering and insulin-sensitizing effects was associated with an immediate induction of typical FGF signaling in liver and adipose tissues and was accompanied by a reduction of hepatic glucose production and an increase in peripheral glucose turnover. The potential metabolic actions of FGF21, such as suppression of hepatic glucose production and stimulation of adipocyte glucose uptake, may have contributed to the observed FGF21 effects.

In *ob/ob* mice, a single dose of FGF21 resulted in a 40–60% decrease in blood glucose, insulin, and amylin levels within 1 h after administration. In DIO mice, FGF21 decreased fasting blood glucose and insulin levels and improved glucose tolerance and insulin sensitivity following a 3-h treatment. Although studies from another laboratory suggest that reduced glucagon secretion may be one of the mechanisms responsible for the antihyperglycemic effect of FGF21 (11), we have not been able to detect FGF21 inhibition of glucagon secretion ex vivo or to observe changes in plasma glucagon levels following FGF21 administration in the previous chronic (25) or current acute studies. We were, however, able to consistently observe a marked reduction in plasma insulin levels following FGF21 injection. In the current study, plasma insulin levels were reduced as quickly as 1 h after FGF21 injection, and the temporal change of plasma insulin levels paralleled that of blood glucose levels. Our data suggest that FGF21 is an insulin sensitizer and that its acute glucose-lowering effect is not mediated through stimulating insulin or suppressing glucagon secretion.

The reduction in insulin levels could result from either a decrease in insulin secretion or an increase in insulin clearance through hepatic extraction or a combination of both. To provide insights into which mechanism was predominant, we measured plasma concentration of amylin, a pancreatic hormone that is cosecreted with insulin from islets with negligible hepatic extraction (8, 20). Plasma amylin levels were reduced to a similar extent and followed a similar time course to that of plasma insulin, suggesting that insulin secretion rather than insulin clearance was largely altered by FGF21 treatment. FGF21 did not appear to have a direct role in inhibiting insulin release when tested in cultured mouse islets. A similar observation was reported in a previous publication from another research group, indicating that FGF21 had a minimal effect on insulin secretion from rat islets although it affected insulin biosynthesis (22). Therefore, the decrease in plasma insulin levels observed in our study likely resulted from improved

peripheral tissue insulin sensitivity and subsequently reduced β-cell compensation. It is yet to be determined what signals communicated from the peripheral tissues to the pancreatic β-cells. Glucose is known as a dominant regulator of insulin release, and a decrease in plasma glucose concentration has been shown to have an immediate inhibitory effect on insulin secretion (4, 18). Therefore, the reduced insulin secretion was likely due to β-cell sensing of a reduction in blood glucose levels after FGF21 treatment.

The acute improvement in insulin sensitivity was confirmed by a hyperinsulinemic-euglycemic clamp study conducted in DIO mice following a 3-h FGF21 treatment. The glucose infusion rate was increased sixfold in association with a 32% reduction in hepatic glucose production and a 20% increase in whole body glucose turnover. However, when we examined the [^{14}C] 2-DG uptake in insulin-responsive tissues, including white and brown adipose tissues, heart, and skeletal muscle, none of the tissues tested showed statistically significant increases in glucose uptake. It is possible that the assay sensitivity was not sufficient to detect individual tissue responses to an overall modest change in the total glucose turnover rate (20%). Nevertheless, results of the present acute study are consistent with results from our previous 3-wk chronic study conducted in the same animal model with the same 10 mg·kg^{-1}·day^{-1} FGF21 dose (25). In that chronic study, FGF21 increased the glucose infusion rate 30-fold, which was accompanied by an 80% reduction in clamp hepatic glucose production and a 40% increase in whole body glucose turnover. We observed increased glucose uptake in all the tested tissues, including adipose tissue, muscle, and heart. The enhanced effects in the chronic study could be attributed to the subsequent reduction in body weight, body fat mass, and lipid levels in plasma and tissues, which did not occur in our acute paradigm.

FGF21 initiates its action by activating FGF receptors in the presence of a coreceptor, βklotho (17, 26). We were able to detect protein expression of βklotho in liver and adipose tissues but not in skeletal muscle or heart tissues. In agreement with the βklotho tissue expression pattern, following a single injection, FGF21 induced phosphorylation of ERK1/2 in liver and adipose tissues but not in skeletal muscle or heart. The FGF21-stimulated signaling cascades, including FRS2 and ERK1/2 phosphorylation, were also detected in multiple hepatoma-derived cell lines and in differentiated human and mouse adipocytes. The rapid signaling events observed in liver and adipose tissues and the lack of a direct effect on pancreatic islet insulin and glucagon secretion suggest that the acute glucose-lowering and insulin-sensitizing effects of FGF21 may result from its metabolic actions in peripheral tissues such as liver and adipose tissues. FGF21 was able to reduce glucose production in our experiments with H4IIE cells. We also confirmed that FGF21 stimulated glucose uptake in 3T3-L1 adipocytes (11). The typical EC_{50} of FGF21 in these assays was ~1 nM, which was consistent with the observed FGF21 concentrations for which the blood glucose-lowering effects were seen. Therefore, our data suggest that the metabolic actions of FGF21 on liver or adipose tissues may contribute to its glucose-lowering and insulin-sensitizing effects.

The rapid and sustained in vivo pharmacodynamic characteristics of FGF21 suggest that a variety of cellular processes may be involved in the mechanisms of FGF21 action. Unlike peroxisome proliferator-activated receptor-γ agonist and metformin, which

produce insulin-sensitizing effects rather slowly because of transcriptionally mediated mechanisms (19, 23), FGF21 led to rapid insulin sensitization within 1 h. Such acute effects (<1 h) may be mediated through posttranslational events without the requirement of new protein synthesis through modulation of metabolic enzyme activities through kinase- and phosphatase-mediated reactions. Whether FGF21 signaling could functionally replace insulin signaling or whether these two pathways cross-talk in the regulation of glucose metabolism requires further studies in the future. The prolonged effect of FGF21 may be mediated through gene transcript and protein synthesis. FGF21 activates the ERK pathway, which is known to regulate the activities of transcription factors and alter transcription of the genes (14). FGF21 has been shown to increase GLUT1 mRNA expression, which leads to increased glucose uptake in 3T3-L1 adipocytes (11). This has been suggested as a transcription-mediated mechanism, because the glucose uptake was abolished when the protein synthesis inhibitors were added into the culture medium (11). In addition, we also demonstrated that FGF21 has the ability to regulate lipogenic gene expression by reducing the nuclear content of transcription factor sterol regulatory element binding protein-1 (25). Overall, FGF21 may control its activities through a diverse mechanism involving posttranslational and transcriptional regulation.

In conclusion, administration of FGF21 elicited rapid and sustained metabolic effects on lowering blood glucose and improving glucose tolerance and insulin sensitivity in two animal models of insulin resistance. The improved glucose metabolism and insulin sensitivity were possibly associated with the metabolic effects of FGF21 in liver and adipose tissues. The present acute study and our previously published chronic study (25) highlight the importance of FGF21 action on glucose-lowering and insulin sensitization.

REFERENCES

1. **Arner P, Pettersson A, Mitchell PJ, Dunbar JD, Kharitonenkov A, Ryden M.** FGF21 attenuates lipolysis in human adipocytes—a possible link to improved insulin sensitivity. *FEBS Lett* 582: 1725–1730, 2008.
2. **Bottcher RT, Niehrs C.** Fibroblast growth factor signaling during early vertebrate development. *Endocr Rev* 26: 63–77, 2005.
2a. **Cryer P.** Glucose homeostasis and hypoglycemia. In: *Williams Textbook of Endocrinology* (10th ed.), edited by Larsen PR, Kronenberg HM, Melmed S, Polonsky KS. Philadelphia, PA: Saunders, 2003.
3. **Dostalova I, Haluzikova D, Haluzik M.** Fibroblast growth factor 21: a novel metabolic regulator with potential therapeutic properties in obesity/type 2 diabetes mellitus. *Physiol Res/Academia Scientiarum Bohemoslovaca* 58: 1–7, 2009.
4. **Gerich JE, Charles MA, Grodsky GM.** Characterization of the effects of arginine and glucose on glucagon and insulin release from the perfused rat pancreas. *J Clin Invest* 54: 833–841, 1974.
5. **Goetz R, Beenken A, Ibrahimi OA, Kalinina J, Olsen SK, Eliseenkova AV, Xu C, Neubert TA, Zhang F, Linhardt RJ, Yu X, White KE, Inagaki T, Kliewer SA, Yamamoto M, Kurosu H, Ogawa Y, Kuro-o M, Lanske B, Razzaque MS, Mohammadi M.** Molecular insights into the klotho-dependent, endocrine mode of action of fibroblast growth factor 19 subfamily members. *Mol Cell Biol* 27: 3417–3428, 2007.
6. **Inagaki T, Dutchak P, Zhao G, Ding X, Gautron L, Parameswara V, Li Y, Goetz R, Mohammadi M, Esser V, Elmquist JK, Gerard RD, Burgess SC, Hammer RE, Mangelsdorf DJ, Kliewer SA.** Endocrine regulation of the fasting response by PPARalpha-mediated induction of fibroblast growth factor 21. *Cell Metab* 5: 415–425, 2007.
7. **Itoh N, Ornitz DM.** Evolution of the Fgf and Fgfr gene families. *Trends Genet* 20: 563–569, 2004.
8. **Kahn SE, D'Alessio DA, Schwartz MW, Fujimoto WY, Ensinck JW, Taborsky GJ Jr, Porte D Jr.** Evidence of cosecretion of islet amyloid polypeptide and insulin by beta-cells. *Diabetes* 39: 634–638, 1990.
9. **Kharitonenkov A, Dunbar JD, Bina HA, Bright S, Moyers JS, Zhang C, Ding L, Micanovic R, Mehrbod SF, Knierman MD, Hale JE, Coskun T, Shanafelt AB.** FGF-21/FGF-21 receptor interaction and activation is determined by betaKlotho. *J Cell Physiol* 215: 1–7, 2008.
10. **Kharitonenkov A, Shanafelt AB.** FGF21: a novel prospect for the treatment of metabolic diseases. *Curr Opin Investig Drugs* 10: 359–364, 2009.
11. **Kharitonenkov A, Shiyanova TL, Koester A, Ford AM, Micanovic R, Galbreath EJ, Sandusky GE, Hammond LJ, Moyers JS, Owens RA, Gromada J, Brozinick JT, Hawkins ED, Wroblewski VJ, Li DS, Mehrbod F, Jaskunas SR, Shanafelt AB.** FGF-21 as a novel metabolic regulator. *J Clin Invest* 115: 1627–1635, 2005.
12. **Kharitonenkov A, Wroblewski VJ, Koester A, Chen YF, Clutinger CK, Tigno XT, Hansen BC, Shanafelt AB, Etgen GJ.** The metabolic state of diabetic monkeys is regulated by fibroblast growth factor-21. *Endocrinology* 148: 774–781, 2007.
13. **Kim HJ, Higashimori T, Park SY, Choi H, Dong J, Kim YJ, Noh HL, Cho YR, Cline G, Kim YB, Kim JK.** Differential effects of interleukin-6 and -10 on skeletal muscle and liver insulin action in vivo. *Diabetes* 53: 1060–1067, 2004.
14. **Kyosseva SV.** Mitogen-activated protein kinase signaling. *Int Rev Neurobiol* 59: 201–220, 2004.
15. **Lacy PE, Kostianovsky M.** Method for the isolation of intact islets of Langerhans from the rat pancreas. *Diabetes* 16: 35–39, 1967.
16. **Nishimura T, Nakatake Y, Konishi M, Itoh N.** Identification of a novel FGF, FGF-21, preferentially expressed in the liver. *Biochim Biophys Acta* 1492: 203–206, 2000.
17. **Ogawa Y, Kurosu H, Yamamoto M, Nandi A, Rosenblatt KP, Goetz R, Eliseenkova AV, Mohammadi M, Kuro-o M.** BetaKlotho is required for metabolic activity of fibroblast growth factor 21. *Proc Natl Acad Sci USA* 104: 7432–7437, 2007.
19. **Reginato MJ, Lazar MA.** Mechanisms by which Thiazolidinediones Enhance Insulin Action. *Trends Endocrinol Metab* 10: 9–13, 1999.
20. **Rink TJ, Beaumont K, Koda J, Young A.** Structure and biology of amylin. *Trends Pharmacol Sci* 14: 113–118, 1993.
21. **Szebenyi G, Fallon JF.** Fibroblast growth factors as multifunctional signaling factors. *Int Rev Cytol* 185: 45–106, 1999.
22. **Wente W, Efanov AM, Brenner M, Kharitonenkov A, Koster A, Sandusky GE, Sewing S, Treinies I, Zitzer H, Gromada J.** Fibroblast growth factor-21 improves pancreatic beta-cell function and survival by activation of extracellular signal-regulated kinase 1/2 and Akt signaling pathways. *Diabetes* 55: 2470–2478, 2006.
23. **Wiernsperger NF, Bailey CJ.** The antihyperglycaemic effect of metformin: therapeutic and cellular mechanisms. *Drugs* 58, *Suppl* 1: 31–39; discussion 75–82, 1999.
24. **Wild S, Roglic G, Green A, Sicree R, King H.** Global prevalence of diabetes: estimates for the year 2000 and projections for 2030. *Diabetes Care* 27: 1047–1053, 2004.
25. **Xu J, Lloyd DJ, Hale C, Stanislaus S, Chen M, Sivits G, Vonderfecht S, Hecht R, Li YS, Lindberg RA, Chen JL, Jung DY, Zhang Z, Ko HJ, Kim JK, Veniant MM.** Fibroblast growth factor 21 reverses hepatic steatosis, increases energy expenditure, and improves insulin sensitivity in diet-induced obese mice. *Diabetes* 58: 250–259, 2009.
26. **Yie J, Hecht R, Patel J, Stevens J, Wang W, Hawkins N, Steavenson S, Smith S, Winters D, Fisher S, Cai L, Belouski E, Chen C, Michaels ML, Li YS, Lindberg R, Wang M, Veniant M, Xu J.** FGF21 N- and C-termini play different roles in receptor interaction and activation. *FEBS Lett* 583: 19–24, 2009.